Available online at www.sciencedirect.com

SciVerse ScienceDirect

Mathematics and Computers in Simulation 91 (2013) 119–133

MATHEMATICS AND COMPUTERS IN SIMULATION

www.elsevier.com/locate/matcom

Original article

Power flow Petri Net modelling for building integrated multi-source power system with smart grid interaction

B.C. Wang, M. Sechilariu *, F. Locment

University of Technology of Compiegne, AVENUES-GSU, 60203 Compiegne, France

Received 14 October 2011; received in revised form 4 January 2013; accepted 27 January 2013
Available online 14 February 2013

Abstract

This paper presents an energy management modelling of a multi-source power system composed of photovoltaic (PV) array, storage and power grid connection, and taking into account messages from smart grid. The designed system can supply a tertiary building at the same time as PV may produce energy. The control strategy aims to manage the power flow through the load with respect to its power demand and public grid constraints. The proposed energy management modelling is based on interpreted Petri Nets formalism. The system is tested using a simulation Stateflow model and responds within certain limits. The results show that this approach is valid and can be a solution for the future smart grid communication between buildings and public grid and may contribute to a better balance between production and consumption and future energy management.

Keywords: Energy management; Smart grid; Photovoltaic; Petri Net modelling; Stateflow

1. Introduction

Currently, grid connected renewable energy resources are proposed in most applications for permanent power injection. However, this development leads to grid-connection incidents, which become true technical constraints. The fluctuations in energy demand and renewable power generation, even for few minutes, induce an effort to supplementary setting on conventional units production whose number in operation must grow to ensure this setting. Furthermore, the increased power consumption involves more quality and reliability to regulate electricity flows, less mismatching between electricity generation and consumption, and more integrated renewable energies. Thus, the concept of smart grid is born in recent years. Smart grid could be easily defined as an electricity delivery system, which transports, converts and distributes the power efficiently (from producers to consumers), with some integrated communication and information technology. The main goal of smart grid communication is to assist in balancing the power generation and the power consumption [10].

On the other hand, the very intermittent and random renewable power generation does not participate in technical regulations for public grid connection (setting voltage and frequency, islanding detection, etc.) and behaves as passive

* Corresponding author. Tel.: +33 (0)3 44 23 49 64.
E-mail address: manuela.sechilariu@utc.fr (M. Sechilariu).

0378-4754/$36.00
http://dx.doi.org/10.1016/j.matcom.2013.01.006

electric generator. Renewable and distributed electricity production is now steadily increasing so that their grid integration associated with an energy management system is more necessary than ever [3]. In urban areas, there is a significant development of small plants of decentralized photovoltaic (PV) power production, therefore associated or integrated to buildings. PV energy purchase conditions lead quite naturally these applications to a grid-connected system with a total and permanent energy injection. However, due to the technical constraints related to the absence of the smart grid which should integrate energy management, this development could be restrained by the power back grid capacity.

In response to these technical constraints, research works are being currently carried out on grid integration of renewable energy generation, by developing new supervision strategies like a high level energy management control. In Ref. [7] a distributed energy management solution by means of multi-agent systems is proposed as an application for hybrid power sources. Other studies like Ref. [9] propose an energy management following some operating modes whose design is based on interpreted Petri Nets (PN).

In Ref. [6], a PV active generator producing power according to the smart grid demand is proposed, but high-speed communication is necessary for a real-time power balancing.

The authors of Ref. [11] propose an optimal power flow management with predictions, which separates the rule based energy management strategy and optimal management. An improvement can be achieved as multi-layer control structure, each layer with a different function. Rule-based energy management strategy, interfaced in the basic layer, can develop advanced energy management control with more flexibility.

In this context, for buildings equipped with PV power plant, an alternative solution is the multi-source power local generation, whose produced energy is intended primarily for self-feeding, with a grid connection for further supply in case of need and for sale of excess energy. By means of a smart grid communication device, this system takes into account the availability, needs and vulnerability of the electric grid. This paper focuses on energy management modelling based on interpreted PN for a multi-source power generation with smart grid interaction. This system is designed for tertiary buildings equipped with local renewable electricity sources. Firstly, the overview of the global system is presented as a multi-source power system coupled with a supervision system dedicated to energy management. Then, the behaviour modelling of the supervision and the power system components behaviour modelling (PV generator, storage, public grid and load) are proposed. Finally, numerical simulation results confirm the relevance of such integrated energy management supervision, and allow tracing the steps on the smart grid integration. The continuity and the prospects of this research are given at the end.

2. Global system overview

The global system is composed of a multi-source power local generation in semi-isolated and safety grid configuration, and a supervision system. Fig. 1 shows this configuration.

PV sources, storage and public grid are connected to a common DC voltage bus through their dedicated converters. The DC bus feeds a DC load, which could represent a DC controllable installation of a tertiary building [12]. Concerning the tertiary building loads, we note that it is possible to have electric loads fed directly by DC power. Some examples of this kind of loads are devices based on microprocessors, computer system power supply, switched-mode power supply, electronic ballasts for the fluorescent lighting, variable-frequency drives for the speed variation of the motors that equip the systems of heating, ventilation and air conditioning, lighting, based on light emitting diodes. These examples represent a very important percentage, most of 90%, of tertiary buildings electric loads. These convergent factors recently justified researches on DC power distribution for tertiary buildings [2,13,14]. As many small PV plants are associated or integrated to buildings, it is essential to restructure their use and to improve their performance by an energy management strategy. For distributed PV energy, on-site generation through the proposed global system can be better scaled to match the power needs of end-users who require specified power services and may more easily accept some load shedding. Hence, in goal to reduce multiple energy conversions for certain appliances and to take advantage of the DC renewable electricity generation [15], for tertiary buildings a DC-grid with smart grid communications may be a solution.

As in Ref. [15], the PV produced energy is intended primarily for self-feeding, whence the isolated aspect. In order to obtain a reliable power distribution, this system is safe thanks to the grid connection for a further supply in case of need, and by means of storage who is primarily involved in smoothing the power balance. Excess power can be traded back to the public grid. The power system is designed to ensure continuous supply to the load. The energy management focuses on power balancing with load shedding and takes into account the grid availability by smart grid messages. To

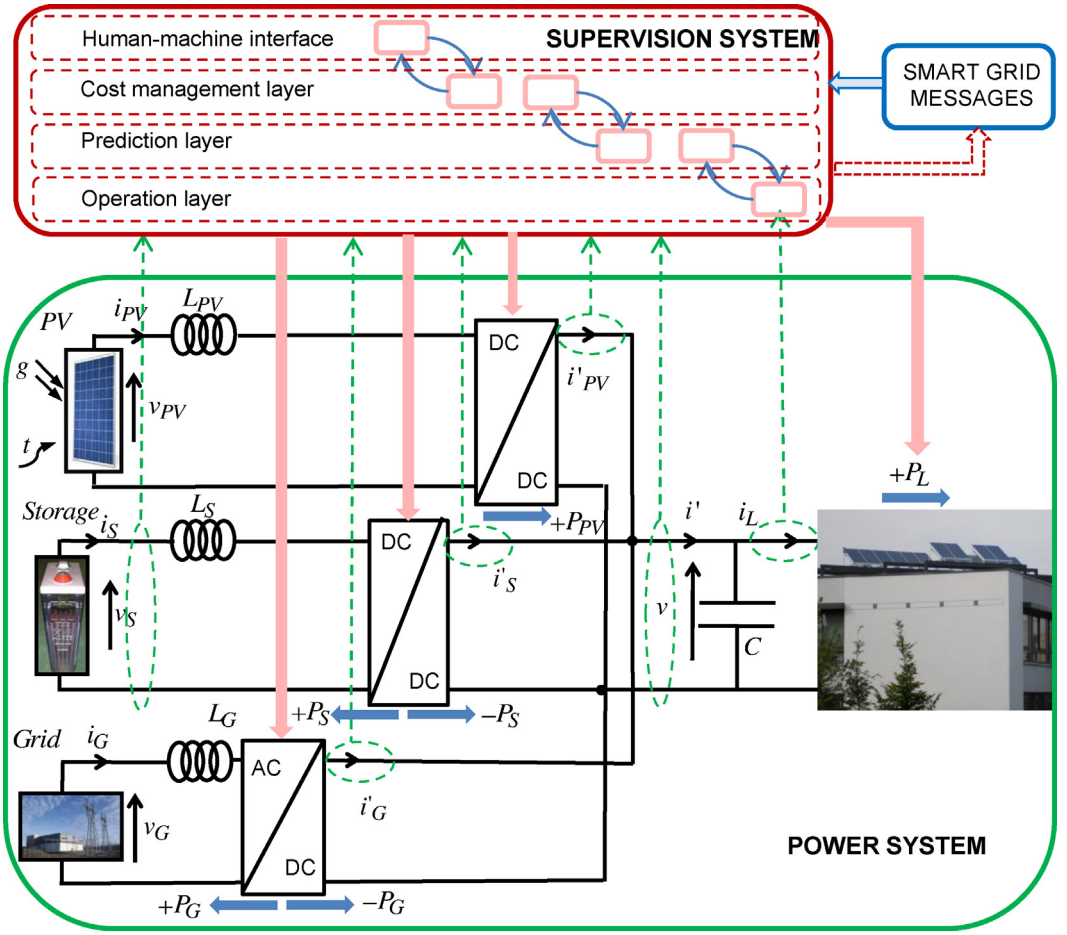

Fig. 1. Global system overview.

easily meet other objectives such as smart grid interaction or energy cost management, the supervision is conceived like a multi-layered system. This is a "bottom-up" approach that permits to communicate with the public grid or with the users without increasing the basic programme implemented in the operational layer.

The described global system can be seen as a hybrid dynamical system defined as system with continuous-time dynamics interacting with discrete-event dynamics. The hybrid behaviour consists of continuous-time power system behaviour controlled by discrete logic/event like circuits switching and supervision system outputs.

2.1. Supervision system

A four-layer supervision architecture is proposed as shown in Fig. 1:

- operation layer which controls the power system for the power balancing and energy control, the main algorithm is implemented in this layer;
- prediction layer which permits the load power limitation estimation;
- cost management layer which can be a main objective;
- human-machine interface layer, which permits interaction with users (operating criteria).

In order to use the full production of the PV energy, with the respect of the grid availability, the supervision system must be able to communicate with the public grid. Hence, by means of a smart grid communication device, the supervision system is informed on the energy price and the limitations of power supply and the power injection

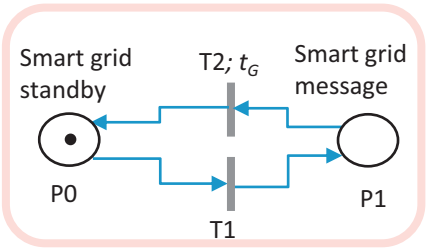

Fig. 2. Smart grid interaction modelling by PN.

at different times; some grid-operating modes could be defined. In addition, this device is able to communicate information, back to the public grid, concerning monitoring and billing purpose. The behavioural modelling of global system is proposed by means of on interpreted PN formalism [1]. The interpreted PN is a powerful graphical and mathematical tool for describing and analyzing different hybrid dynamical systems. A PN graphic contains three kinds of objects: place (state variable), transition (state transformer), token (indicator for active state) and arc. The directed arcs, whose weight is considered to be one in this study, connect places and transitions and indicate the token flow when transition is fired. A transition can be enabled if its upstream or input places have enough tokens according to corresponding arc weights. An enabled transition may fire at any time. As interpreted PN, each transition could have conditions related to it, and transition is fired only if the transition is enabled and its conditions are satisfied. When fired, the tokens in the input places are moved to output places, according to arc weights and place capacities. Starting with an initial marking, given by initial tokens of places, the graph-based structure simulates the dynamic behaviour of a system by continuously firing enabled transitions. Many static and dynamic properties of a PN may be mathematically proven. The basic analysis of PN models is not necessary to be presented in this paper. However, concerning the PN models presented below and in Section 3, using the place-invariants and transition-invariants, we note that the structural verification proves that each model is live (there exists an initial marking for which the PN is live), bounded (tokens limitation for all initial marking), and without deadlocks or conflicts.

The smart grid interaction is modelled with a timed interpreted PN represented by two places (P0 and P1) and two transitions (T1 and T2), as illustrated in Fig. 2. The P0 place represents the smart grid in a standby mode and the P1 place is reached when the operator gives the operating grid mode. This event is the firing condition of the transition T1. After the t_G time, measured in hours from the arrival of the token in place P1, the timed transition T2 can be fired and the supervision system is informed of the switching operating mode instant.

Once the supervision system is informed about the grid-operating mode, it controls the power system according to the specific grid-operating mode and each element constraints. Except the smart grid messages, the other inputs of the supervision system are the storage voltage v_S and the power system status given by: PV power $P_{PV} = i'_{PV}v$, load power $P_L = i_L v$, storage power $P_S = i'_S v$ and grid power $P_G = i'_G v$, where i'_{PV}, i_L, i'_S and i'_G are respectively PV current, load current, storage current and grid current after their dedicated converters, and v is the DC bus voltage. The storage state of charge (SOC) is estimated by measuring the storage voltage v_s. The supervision system outputs control parameters in order to manage or to constrain power flow in power system. The goal is to feed continuously the DC load with a maximum of produced PV energy. The grid connection and the storage can run together or separately, with respect of supervision control. The PV plant and the load are not controllable by the supervision system, but they can be constrained if necessary.

2.2. *Power system control*

The power system continuous-time model is used following [8,15]. The PV model is used following [5]. As this article focuses more on power flow modelling of the system, detailed continuous-time models, which involve the description of each power system component, are not given.

The PV panels work in maximum power point tracking (MPPT) mode using the perturb and observe (P&O) algorithm [5]. By P&O algorithm, P_{PV} changes according to solar irradiation g (W/m^2) and cell temperature t (K). The load power P_L is considered, in this study, according to a building's power lighting demanded by the users (power as arbitrary value). P_L is not controllable but can be limited if necessary. In order to ensure compatibility between the different

elements, a set of inductors, L_{PV}, L_S, L_G, and a capacitor C are introduced as shown in Fig. 1. In a steady state operation, the output voltage v should be constant with the following power balance:

$$P_{PV} = P_S + P_G + P_L \tag{1}$$

By means of a current closed loop control, the grid power P_G and the storage power P_S can be controlled using the corresponding current reference given to power system controller. Thus, the DC bus power adjustment P^* is defined as:

$$\begin{aligned} P^* &= P_{PV} - P_L - k_P(v^* - v) - k_I \int_0^t (v^* - v)\mathrm{d}t \\ P^* &= P_S^* + P_G^* \end{aligned} \tag{2}$$

where P_S^* and P_G^* are respectively the storage power reference and the grid power reference; k_P and k_I are the PI controller parameters, and v^* is the control reference voltage. Concerning the grid power reference, it should be noted that P_G^* does not represent a prescribed power reference, which has been traded 1 day ahead as in usual liberalized electrical market. As in this study the produced energy is intended primarily for self-supply, the grid connection allows complementary power supply when needed and the sale of excess energy. So, the grid power reference is considered as a residual power, which is exchanged with the grid for power balancing purpose.

P_{PV} and P_L are considered as known disturbances for DC bus voltage control, and they are added in this equation to reject disturbances. In Eq. (2) the voltage v^* is imposed, the power P_{PV} is a function of solar irradiance and PV cell temperature, and the P_L is imposed by the DC load. The block diagram of a similar control is given in Ref. [8].

Therefore, as mentioned before, the system should be able to manage powers P_G and P_S. In order to distribute power between storage and grid, a distribution coefficient K_D is introduced. The power distribution is given as:

$$P_S^* = K_D P^*; \quad P_G^* = P^* - P_S^* \tag{3}$$

with $0 \le K_D \le 1$ and taking into account that P_S^* and P_G^* should not exceed the corresponding physical element limitation. In Eq. (3) the storage is considered always available, charge or discharge operating mode. Otherwise, the storage power is $P_S^* = 0$. For given values of K_D, an infinite number of solutions may exist; K_D values could be the result of an energy cost optimization calculus (not developed in this work). For this first approach, the goal is to verify the feasibility of the proposed multi-source energy management. Therefore, the priority is given to the storage system with the respect of the public grid constraints. So, firstly $P_S^* = K_D P^*$ is calculated, then, P_G^* is calculated as $P_G^* = P^* - P_S^*$ with consideration of storage physical limitations, which mean $P_S^* = 0$ if the storage reaches its upper limit or its lower limit.

In the simulation test only two cases are retained, $K_D = 1$ and $K_D = 0.8$.

If $K_D = 1$ then storage is a priority in both charging and discharging mode and $P_S^* = P^*$. Once the storage reaches its upper limit or lower limit, the public grid takes over for the power balancing. So, starting this instant, $P_G^* = P^*$.

For $K_D = 0.8$, which is the second case studied, the P^* is shared between the storage and the public grid. So, $P_S^* = 0.8 \cdot P^*$ and $P_G^* = 0.2 \cdot P^*$. Once the storage reaches its upper limit or lower limit, the public grid takes over for the power balancing and $P_G^* = P^*$.

As the strategy takes account only the constraints imposed by the public grid via the smart grid, e.g. limitations on the power drawn from the grid to the system, if P_G^* is higher than the public grid limitations, then P_G^* becomes equal to the imposed limitation and the load shedding should be operated to meet power balancing.

Further work involves more elaborate strategies and therefore a multitude of possible K_D values corresponding to techno-economic criteria, weather, conditions of use, forecast power demand, etc.

3. Behavioural modelling of power system components

The behavioural modelling of power system components is proposed by means of PN formalism. By identifying possible physical states of the system, this step allows the subsequent design of energy management.

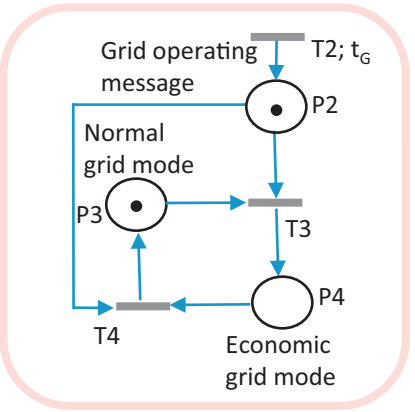

Fig. 3. Grid-operating mode modelling by PN.

3.1. Grid-operating mode modelling

The public grid companies limit the usage of energy in some area during peak-hours consumption period. Another fact is that sometimes the price of electricity could be higher than normal, so people are supposed to use less electricity. These two grid-operation modes are taken into consideration.

In order to illustrate the differences between grid-operating modes, it is assumed that the load has $P_{L\max}$ as contractual subscribed power, and the PV plant has P_{PV_p} as peak power provided by the PV panel manufacturer under industrial standard test conditions (STC) of solar irradiance of 1000 W/m^2 with zero angle of incidence, solar spectrum of 1.5 air mass and 25 °C PV cell temperature. $P_{L\max}$ and P_{PV_p} are constant values. Hence, the grid power evolution for the supply operating mode, P_{G_S}, is defined as $-P_{G\_S\_\lim} \le P_{G\_S} \le 0$, with $P_{G\_S\_\lim} \le P_{L\max}$. The $P_{G\_S\_\lim}$ is imposed by the grid-operating mode. Regarding the injection operating mode, the injected grid power P_{G_I} evolution is defined as $0 \le P_{G\_I} \le P_{G\_I\_\lim}$. The injected power may have constrained limits, but, in order to simplify our model at this primary step, it is assumed that there is no imposed injection limit and. The two grid-operating modes are:

- Normal grid-operating: $P_{G\_S\_\lim} = P_{L\max}$ and $P_{G\_I\_\lim} = P_{PV\_p}$. The load may use maximum power $P_{L\max}$ from grid, and the system may inject the maximum power into the grid. In addition, energy price is normal.
- Economic grid-operating: $P_{G\_S\_\lim} = 0.8P_{L\max}$ and $P_{G\_I\_\lim} = P_{PV\_p}$. The load can use maximum power $P_{L\max}$ from grid, but energy price is normal only for the part less or equal to $0.8P_{L\max}$. For the part that exceeds $0.8P_{L\max}$, the energy price becomes higher. The user is encouraged to use less than $0.8P_{L\max}$. The system may inject maximum power into the grid. In this work, the economic operating mode is: the demanded load power P_{LD} from the grid is strictly limited to maximum $0.8P_{L\max}$, and the grid connection will be cut off if the demand exceeds the limit.

The grid PN model is shown in Fig. 3 and definitions of places, which are associated with the grid-operating modes, are given in Table 1.

Table 1
Definitions for grid PN model.

Name	Description
P2	Grid-operating message after t_G
P3	$0 \le P_{G\_I} \le P_{PV\_p}$ and $-P_{L\max} \le P_{G\_S} \le 0$
P4	$0 \le P_{G\_I} \le P_{PV\_p}$ and $-0.8P_{L\max} \le P_{G\_S} \le 0$
T3	T3 is enable if P2 and P3 are both occupied with token
T4	T4 is enable if P2 and P4 are both occupied with token

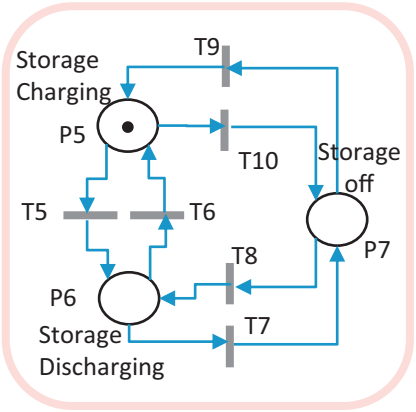

Fig. 4. Storage-operating mode modelling by PN.

As the smart grid gives information about the grid-operating mode, this message is regarded as an event associated with the T2 transition. Moreover, the switching operating mode event will occur after the time t_G. In this model, the T3 and T4 firing conditions are given only by the token presence in upstream places.

3.2. Storage operating mode modelling

The storage is able to charge and discharge when its voltage v_S is in normal range $V_{S\min} \leq v_S \leq V_{S\max}$, with $V_{S\min}$ and $V_{S\max}$ representing respectively the minimum and maximum voltage limitations for storage operation. The SOC variable is used to indicate the storage level, with $SOC = 0$ when $v_S = V_{S\min}$ and $SOC = 1$ for $v_S = V_{S\max}$ when maximum voltage is reached. Three operating modes of the storage are modelled by PN and are shown in Fig. 4.

Definitions of places and transitions firing conditions are given in Table 2.

3.3. PV operating mode modelling

In order to operate a PV plant at its maximum power point, whatever the solar irradiance and cell temperature variations, a MPPT method is needed to find and maintain the maximum power. This strategy aims to find the voltage or current on which the PV plant provides the maximum output power. In this study, the P&O algorithm is used to impose the current reference. When there is no enough solar irradiation or no power demanded by the other elements, PV plant is turned off and $P_{PV} = 0$, otherwise it is supposed to work in MPPT mode with $P_{PV} = P_{PV\_MPPT}$, where P_{PV_MPPT} is the maximum PV power which can be extracted under a given solar irradiance and PV cell temperature. Hence, two PV operating modes are considered in this study and the PN model is shown in Fig. 5 with the definitions given in Table 3. The supervision system turns off the PV plant when conditions are met.

Table 2
Definitions for storage PN model.

Name	Description
P5	Charging operating mode
P6	Discharging operating mode
P7	Storage turn off
T5	$v_S > V_{S\min}$ and $P_{PV} < P_L$
T6	$v_S < V_{S\max}$ and $P_{PV} > P_L$
T7	$v_S \leq V_{S\min}$
T8	$v_S > V_{S\min}$ and $P_{PV} < P_L$
T9	$v_S < V_{S\max}$ and $P_{PV} > P_L$
T10	$v_S \geq V_{S\max}$

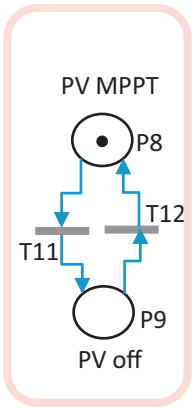

Fig. 5. PV-operating mode modelling by PN.

Table 3
Definitions for PV PN model.

Name	Description
P8	$P_{PV} = P_{PV\_MPPT}$
P9	$P_{PV} = 0$
T11	$P_{PV} = 0$ or $(P_{G\_I\_\lim} = 0$ and $P_L = 0$ and $v_S \geq V_{S\max})$
T12	$P_{PV} \neq 0$

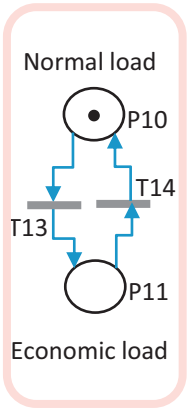

Fig. 6. Load-operating mode modelling by PN.

Table 4
Definitions for load PN model.

Name	Description
P10	$0 \leq P_L \leq P_{L\max}$
P11	$0 \leq P_L \leq 0.8P_{L\max}$
T13	$v_S \leq V_{S\min}$ and $(P_{G\_S\_\lim} + P_{PV} < P_{L\max})$
T14	$P_{G\_S\_\lim} + P_{PV} \geq P_{L\max}$

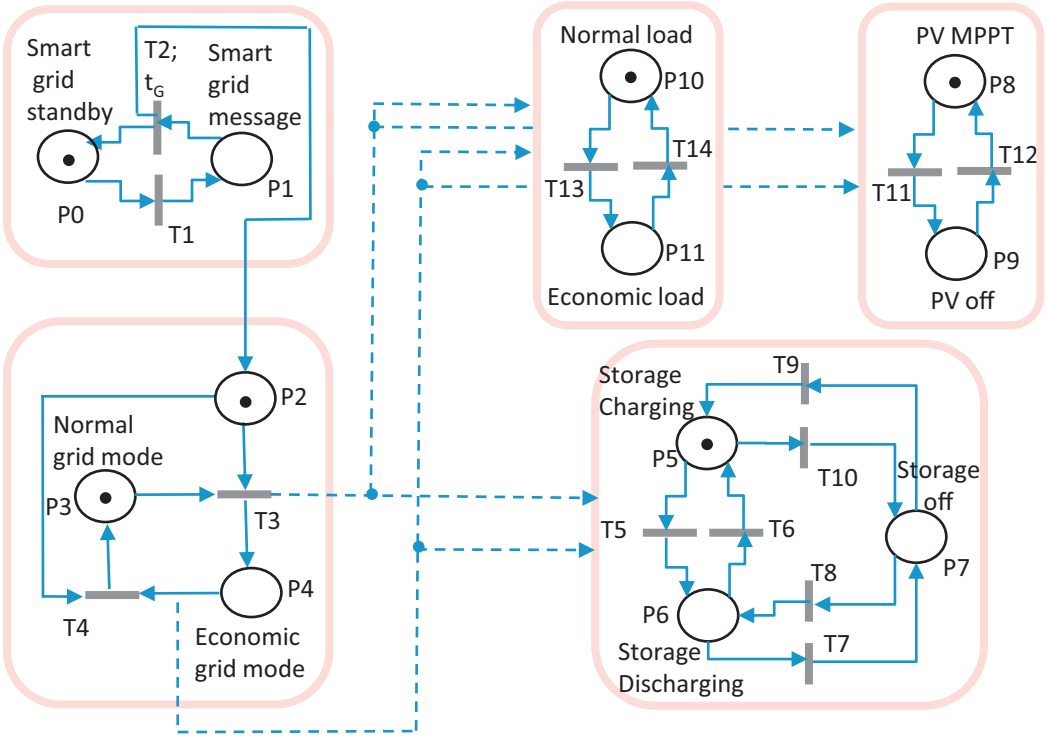

Fig. 7. Energy management modelling by PN.

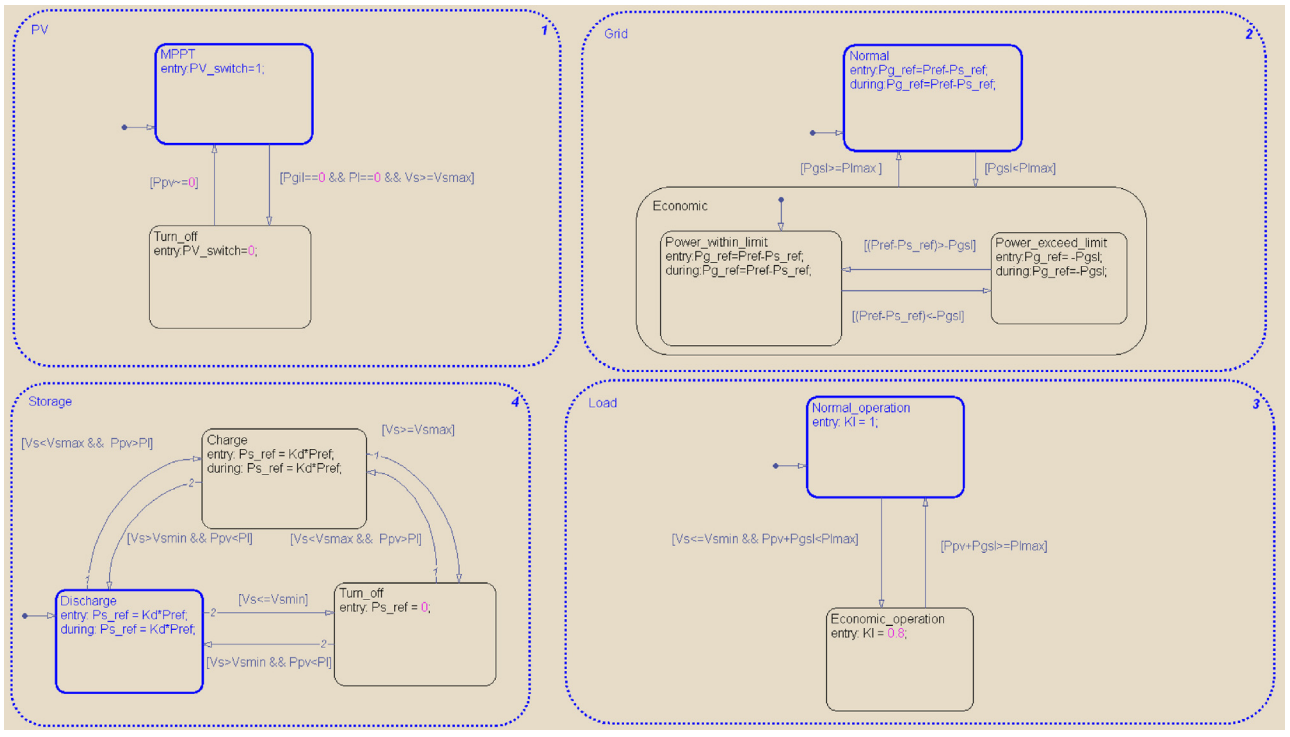

Fig. 8. Energy management Stateflow diagram (screen-printing during simulation).

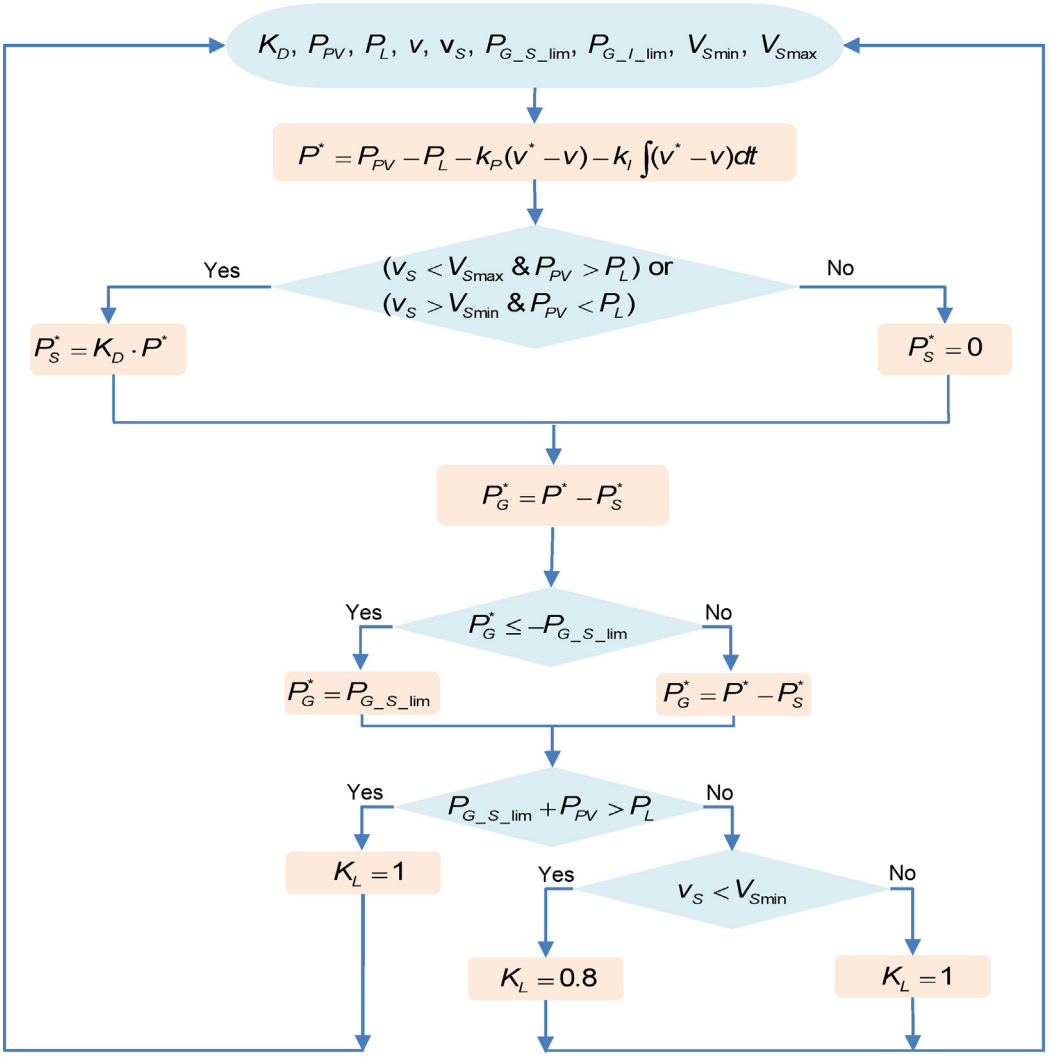

Fig. 9. Energy management strategy diagram.

3.4. Load operating mode modelling

Concerning the load, a limited power P_{L_lim} is introduced to restrict the load power demand. The PN model of the load is shown in Fig. 6. Two operating modes are taken into account:

- Normal load operation: $0 \le P_L \le P_{Lmax}$. The load can demand the maximum P_{Lmax} power.
- Economic load operation: $0 \le P_L \le P_{L\_lim}$. The demand can reach a limited power P_{L_lim}. In this work $P_{L\_lim} = 0.8P_{Lmax}$. Therefore, in this case, if the load power is $P_L > 0.8P_{Lmax}$, the building lighting system must turn off some lights, which were prior defined in order to ensure supply of the other lights.

The definitions of places and transitions firing conditions are given in Table 4. In order to describe the limit imposed to the load, despite system scale for different building applications, the coefficient $K_L = P_{L\_lim}/P_{Lmax}$ is defined. The supervision output system uses K_L to constrain the load power when there is not enough energy to supply the load, or the grid energy is not enough cheap. Many values of K_L could be introduced, but in this study there are only two, $K_L = 1$ and $K_L = 0.8$, representing respectively the normal and economic load mode. In Section 5, the load power simulation analysis leads to use two variables: the load constrained power P_{LC} and the load demanded power P_{LD}.

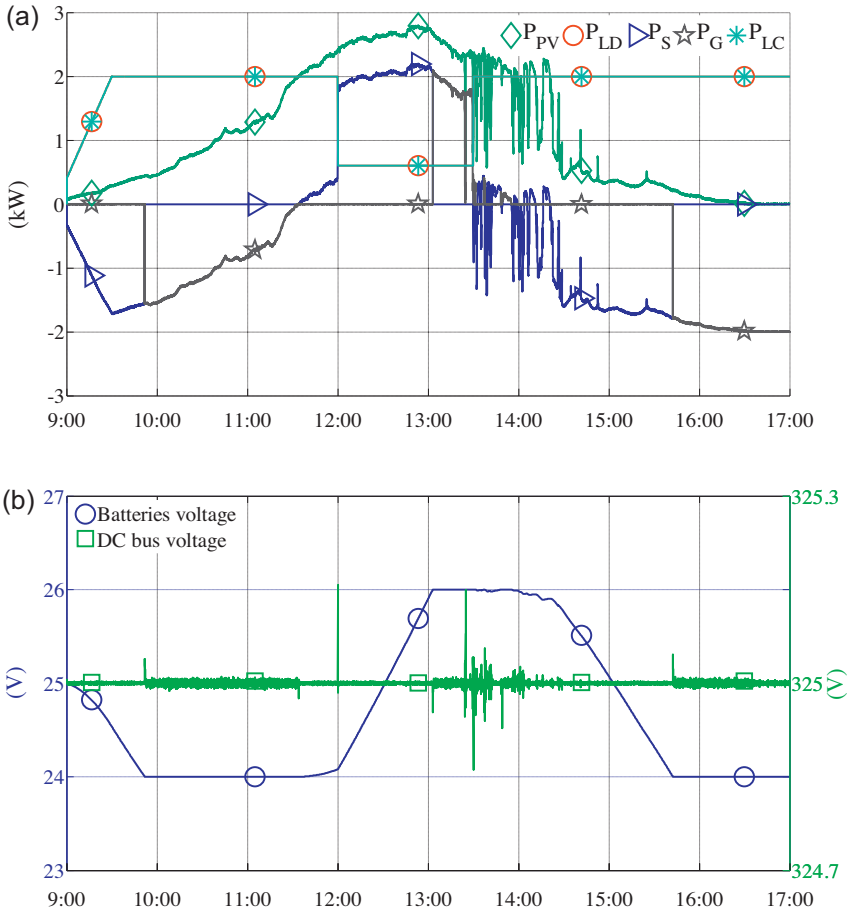

Fig. 10. Power (a) and voltage (b) profiles for $K_D = 1$ and normal grid-operating mode.

4. Energy management modelling

As explained in Section 2.1, a four-layer control structure has been used for the design of the supervision. The user's interface helps to design the graphical monitoring of the system and gives the operating criterion. This operating criterion is assumed to be normal for building power self-feeding with respect of storage availability. In this primary step the users interface is not developed. After optimization calculation using specifically metadata, the cost management layer should be able to inform the operation layer about the K_D value. The operation layer, through the implemented algorithm, calculates P_S^* and P_G^* with the respect of their limitations, and gives the value of K_L to the prediction layer.

The energy management communication inside and between layers of supervision is modelled using PN (Fig. 7). Let us suppose that the grid is in normal operating mode, the PV plant is in MPPT operating mode, the storage is in charging mode, and the smart grid is sending the message to announce the grid-operating mode switching (token in all respective places as initial marking). Thus, the T1 transition is fired and a token arrives in place P1. After t_G time, the T2 is fired and P2 wins a token. Place P4 is empty, thus the transition T4 is not enabled. As place P3 is already occupied by token, places P2 and P3 enable T3, whose firing moves these tokens from the input places P2 and P3 in the output place P4. That is the moment when the grid-operating mode is switched, the place P4 is occupied by a token and the supervision operational layer is informed of grid power limits $P_{G\_S\_\mathrm{lim}}$ and $P_{G\_I\_\mathrm{lim}}$. This information is taken into account in Eq. (3) for the power balancing control. Concerning the load, that could be possible but not immediately required to switch in economic mode. This happen only if the T13 firing conditions are true. In this case, the prediction layer transmits the coefficient $K_L = 0.8$ to the real load shedding device.

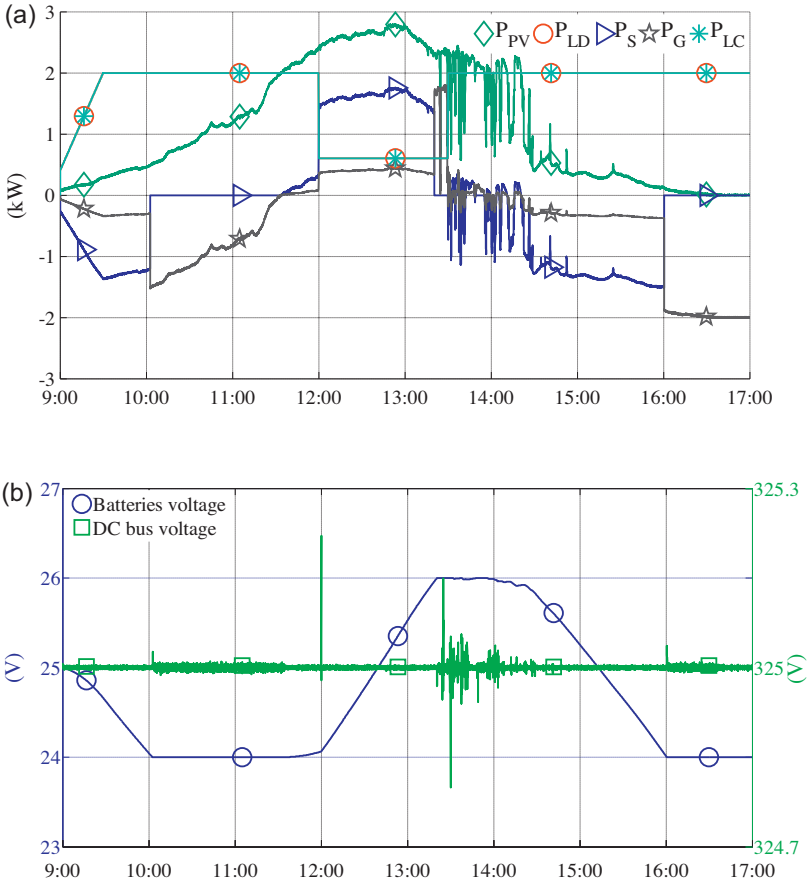

Fig. 11. Power (a) and voltage (b) profiles for $K_D = 0.8$ and normal grid-operating mode.

The described system has a hybrid aspect from the higher level, which is supervision, to the lower one, which is local control. The continuous and discrete aspects coexist and interact with each other. As method for validating such models, the hybrid simulation is proposed. It is based on the connection and interaction of two submodels that continuous and discrete simulation progress in alternation. Continuous simulation takes care of the continuous dynamic and is executed while no event has been detected. The main problem of the hybrid simulation is the synchronization between the two submodels.

In this study, in order to perform numerical hybrid simulation tests, Simulink and Stateflow development of MATLAB environment are proposed. Simulink helps to model the continuous dynamics of the system and Stateflow is used to specify the discrete control logic and the modal behaviour of the system. Stateflow design language is based on the concept of hierarchical automata from Statecharts [4] and allows developing PN model through the approximation made between states/places and switching/firing transitions conditions. Thus, the proposed energy management strategy modelled by PN is translated into Stateflow charts model. Fig. 8 shows discrete state system simulation by Stateflow in the MATLAB environment during its interaction with Simulink (screen-printing where active states are highlighted).

The continuous dynamics of the system are operated by the operation layer, through an implemented algorithm, that calculates reference power values P_S^* and P_G^* following Eqs. (2) and (3), with the respect of their limitations, and gives the value of K_L. The energy management algorithm flowchart is presented in Fig. 9. This algorithm focuses on the power system control. For this first approach, the priority is given to the storage system, thus $P_S^* = K_D P^*$. In the other hand, in order to respect the utility grid availability, if the calculated P_G^* is higher than the limit imposed by the smart grid, then $P_G^* = P_{G\_S\_\lim}$ and a load shedding could be imposed, as $K_L = 0.8$, depending on P_{PV} value and the storage availability.

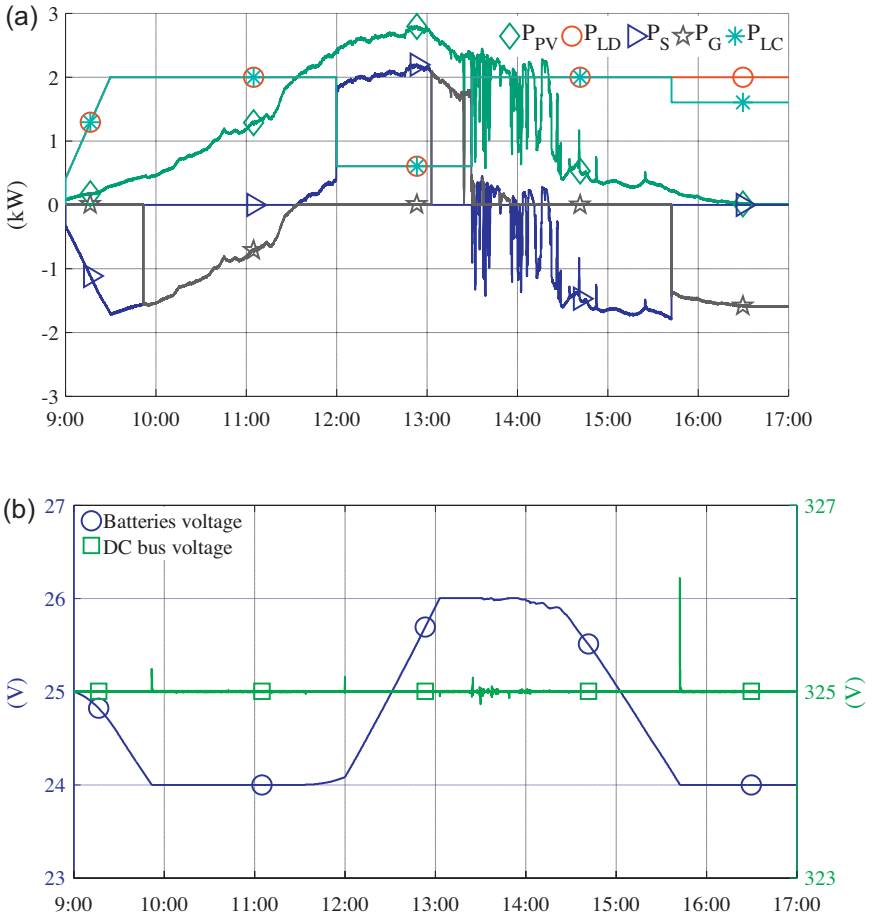

Fig. 12. Power (a) and voltage (b) profiles for $K_D = 1$ and economic grid-operating mode.

5. Simulation results and analysis

The objective of this work is to validate a comprehensive approach rather than purely numerical results. For this reason, we do not give the numerical values of various system components studied. The PV model is used to produce specified power according to weather conditions. The utility grid emulator is an ideal AC power source electrically coupled to the DC bus through power converter legs. Storage is modelled as a capacitor with 88 Ah capacity between 24 V and 26 V. Load is an arbitrary power profile which can be shed, that could represent house lighting which imposes the values of DC bus voltage and the load current. The DC bus is modelled as capacitor. As stated in Section 2.2, detailed continuous-time models are described in Ref. [5,8,15]. The simulation results were obtained under the MATLAB-Simulink and Stateflow environment. MATLAB-Simulink, as a continuous simulator reference, permit powerful modelling of the continuous part of the system and Stateflow specifies its discrete behaviour. Following the Stateflow model, Simulink features a stateflow library with which it is possible to encode graphically the behaviour of each power system component. The MATLAB-Simulink model concerns the physical model of the power system components and is relatively simple.

The implemented automatic control described earlier works satisfactorily. For the period taken into account, from Figs. 10–13 it is observed that the strategy outlined earlier is well respected at all times. For $P_{PV} > P_L$, the storage system receives energy, in contrast it supplies. The storage charge discharge system has priority over the public grid. Once the storage has reached its limits, upper or lower voltage limit, the public grid takes over. For $K_D = 1$, the storage cycles are not operated at same time with the grid. In contrast, they could work together for $K_D = 0.8$.

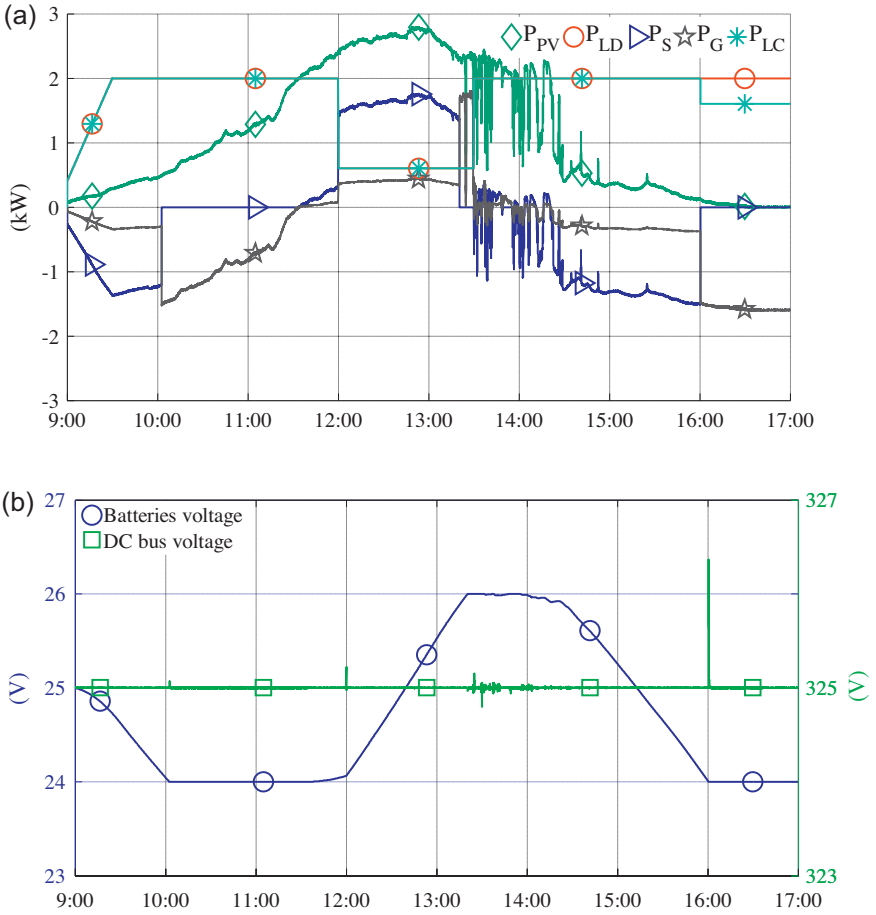

Fig. 13. Power (a) and voltage (b) profiles for $K_D = 0.8$ and economic grid-operating mode.

In order to be economically profitable, an optimal DC bus voltage value to adopt may be 325VDC [14]. Concerning DC bus, it is shown in Figs. 10(b)–13(b) that the voltage remains at a constant value 325 V. The DC bus constant voltage proves the power flow stability during the power balance. The DC bus stability is satisfactory with voltage's fluctuation less than 0.50% of the rated DC bus voltage. The most significant fluctuation during the dynamic process can be observed in Fig. 12(b) and Fig. 13(b), around 15:40. In this case, the storage reaches the lower voltage limit 24 V and the grid takes over. However, the voltage controller is able to make the DC bus voltage steady with a very light fluctuation which could be improved by means of a better controller tuning, if required by the experiment test.

Figs. 10(a) and 11(a) concern normal grid-operating mode. Thus, the load does not need to be switched in economic mode and the power demanded by the load P_{LD} is identical to the power load constrained P_{LC} by the system.

In Figs. 12(a) and 13(a) the economic grid-operating mode imposes $P_{G\_S\_\mathrm{lim}} = 0.8P_{L\mathrm{max}}$. Hence, when PV does not provide sufficient energy and the storage is empty, the system constraints the load power. The load switches to economic mode $P_{LC} = 0.8P_{L\mathrm{max}}$.

6. Conclusion

Integrated renewable electricity and smart grid interaction concern both the utility companies and the end-users. In the next 10 years, the smart grid could concern tertiary and residential buildings with power "routers", whose goal is to manage the real time power demand in order to adjust the electricity generation. For end user this device could control energy use, operating hours and pricing.

In order to achieve a better grid integration of renewable energy, in urban areas, this study proposes a semi-isolated and safety system for self-feeding of buildings equipped with renewable electricity. In this work, a simple and quick to implement energy strategy is applied. This strategy was not necessarily developed to improve global efficiency or life cycle of the storage system, but was rather intended to design energy management supervision for a multi-source power system including PV, storage and grid-connection.

According to the message received from the smart grid, the energy management system takes into account the power grid limitation, calculates the power reference of storage and grid, and constraints the load if necessary. Simulation results validate the design of the whole system and the proposed energy management. The next step is the implementation in our experimental PV platform.

The major technical contribution of this paper is linked to the proposed control design that permits better PV production grid integration with load shedding and respects grid supply limitations to reduce grid peak consumption. Also, the control provides interface for optimizing local power flow to reduce negative impact on the utility grid and to reduce energy cost. The modelling and simulation of the system provide discrete event analysis and facilitate the system design.

In further work, predictions and uncertainties on power sources and load request will be considered and efficiency of energy conversion will be studied. Multicriteria optimization related to the risk of discrepancy between the PV energy production, grid availability and load management prediction should permit the calculation of K_D.

References

[1] R. David, H. Alla, Discrete, Continous, and Hybrid Petri Nets, 2nd ed., Springler-Verlag, Berlin, 2010.
[2] K. Engelen, E. Leung Shun, P. Vermeyen, I. Pardon, R. D'hulst, J. Driesen, R. Belmans, The feasibility of small-scale residential dc distribution systems, in: Proceedings of the 32nd Annual Conference of the IEEE Industrial Electronics, IECON 2006, 6–10 November, Paris, France, 2006, pp. 2618–2623.
[3] Y. Gurkaynak, A. Khaligh, Control and power management of a grid connected residential photovoltaic system with plug-in hybrid electric vehicle (PHEV) load, in: Proceedings of IEEE Applied Power Electronics Conference and Exposition, APEC 2009, 15–19 February, Washington, DC, USA, 2009.
[4] D. Harel, Statecharts: a visual formalism for complex systems, in: Science Computer Program, Technical Report 8, The Weizmann Institute of Science, Rehovot, Israel, 1987, pp. 231–247.
[5] I. Houssamo, F. Locment, M. Sechilariu, Maximum power tracking for photovoltaic power system: development and experimental comparison of two algorithms, Renewable Energy 35 (10) (2010) 2381–2387.
[6] H. Kanchev, D. Lu, F. Colas, V. Lazarov, B. François, Energy management and operational planning of a microgrid with a PV-based active generator for smart grid applications, IEEE Transactions on Industrial Electronics 58 (10) (2011) 4583–4592.
[7] J. Lagorse, D. Paire, A. Miraoui, A multi-agent system for energy management of distributed power sources, Renewable Energy 35 (1) (2010) 174–182.
[8] F. Locment, M. Sechilariu, I. Houssamo, DC load and batteries control limitations for photovoltaic systems. Experimental validation, IEEE Transactions on Power Electronics 27 (9) (2012) 4030–4038.
[9] D. Lu, H. Fakham, T. Zhou, B. François, Application of Petri Nets for the energy management of a photovoltaic based power station including storage units, Renewable Energy 35 (6) (2010) 1117–1124.
[10] E. Peeters, R. Belhomme, C. Batlle, F. Bouffard, S. Karkkainen, D. Six, M. Hommelberg, ADDRESS: scenarios and architecture for active demand development in the smart grid of the future, in: Proceedings of CIRED 20th International Conference on Electricity Distribution, 8–11 June, Prague, Czech Republic, 2009.
[11] Y. Riffonneau, S. Bacha, F. Barruel, S. Ploix, Optimal power flow management for grid connected PV systems with batteries, IEEE Transactions on Sustainable Energy 2 (3) (2011) 325–332.
[12] M. Robinson, Enhancing reliability and efficiency using locally generated DC power – the hybrid building, in: Proceedings of the West Coast Energy Management Congress, WCEMC'05, 28–29 June, San Diego, USA, 2005.
[13] D. Salomonsson, A. Sannino, Low-voltage DC distribution system for commercial power systems with sensitive electronic loads, IEEE Transactions on Power Delivery 22 (3) (2007) 1620–1627.
[14] A. Sannino, G. Postiglione, M. Bollen, Feasibility of a DC network for commercial facilities, IEEE Transactions on Industry Applications 39 (5) (2003) 1499–1507.
[15] M. Sechilariu, F. Locment, I. Houssamo, Multi-source power generation system in semi-isolated and safety grid configuration for buildings, in: Proceedings of IEEE Mediteranean Electrotechnical Conference MELECON 2010, 25–28 April, La Valletta, Malta, 2010.